International Journal of Applied Earth Observation and Geoinformation 12S (2010) S63–S68

Contents lists available at ScienceDirect

International Journal of Applied Earth Observation and Geoinformation

journal homepage: www.elsevier.com/locate/jag

Image mining for drought monitoring in eastern Africa using Meteosat SEVIRI data

Coco M. Rulinda *, Wietske Bijker, Alfred Stein

International Institute for Geo-Information Science and Earth Observation (ITC), Department of Earth Observation Science, Hengelosestraat 99, P.O. Box 6, 7500 AA Enschede, The Netherlands

ARTICLE INFO

Article history:
Received 20 November 2008
Accepted 16 October 2009

Keywords:
Image mining
NDVI
Vegetation monitoring
Drought
Meteosat SEVIRI
Eastern Africa

ABSTRACT

We propose an image mining approach to monitor drought using Meteosat Spinning Enhanced Visible and InfraRed Imager (SEVIRI) image data. SEVIRI image data provide frequent Normalized Difference Vegetation Index (NDVI) time series which are important to assess the evolution of drought conditions. Vegetation condition is characterized in space by the deviation of the current NDVI observations at locations from their temporal mean values. In this paper we assume a gradual evolution of vegetation stress caused by drought and hence address this aspect with the use of a membership function applied to vegetation stress values to model drought. Our approach is implemented on subset image data of eastern Africa. Vegetated sites in a drought prone area of the region serve as an illustration using the drought spell at the end of 2005. This study shows that the use of a membership function allows capturing the gradual evolution of drought and can be used to model drought from observed vegetation conditions.

1. Introduction and background

Drought is defined as an extended period of abnormally dry weather that causes water shortage and damage to vegetation. It is a creeping and recurrent natural phenomenon and its impacts, covering large areas, can last for weeks or months (Wilhite, 2005). The onset, duration and severity of droughts are often difficult to determine and their characteristics may vary significantly from one region to another. In systems reliant on rainfall as the sole source of moisture for crop or pasture growth, seasonal rainfall variability is inevitably mirrored in both highly variable production levels as well as in the risk-averse livelihoods (Cooper et al., 2008).

Africa has a long history of rainfall fluctuations of varying lengths and intensities (Nicholson, 1994, 2000). At different spatial and temporal scales, studies showed different behavior of rainfall trends in Africa; while studies by Olsson et al. (2005) and Herman et al. (2005) showed an increase of rainfall and greenness in parts of the Sahel region, Swenson and Wahr (2009) showed a decrease of water shortage in eastern Africa between 2003 and 2008 where drought and famine situations were periodically reported (FEWSN, 2005c, 2006b).

Drought has particularly negative impacts on agricultural production in the eastern African region, as most of agriculture is dependent on rainfall (Barron et al., 2003; Slegers, 2008; Thorton et al., 2009). In this study we focus on monitoring the impacts of drought on vegetation, referred to as *vegetative drought*, using a membership function applied to Meteosat Spinning Enhanced Visible and Infrared Imager (SEVIRI) data.

1.1. Vegetation index

Satellite vegetation monitoring involves the exploitation of information from the red and near-infrared wavelengths combined into the Normalized Difference Vegetation Index (NDVI) (Tucker, 1979). NDVI is calculated as in Eq. (1):

$$\mathrm{NDVI} = \frac{\lambda_{\mathrm{NIR}} - \lambda_{\mathrm{RED}}}{\lambda_{\mathrm{NIR}} + \lambda_{\mathrm{RED}}} \tag{1}$$

where λ_{NIR} and λ_{RED} are the spectral reflectance in the near infrared (0.75–1.1 μm) and red (0.4–0.7 μm) respectively. NDVI is the most commonly used vegetation index and has been shown to be related to vegetation vigor, percentage green cover and biomass (Myneni and Asrar, 1994; Anyamba and Tucker, 2003; Tucker and Stenseth, 2005). It is a non-linear function that varies between −1 and +1, and is undefined when both λ_{NIR} and λ_{RED} are zero. NDVI values for vegetated land areas generally range from approximately 0.1 to 0.7, with values greater than 0.5 indicating dense vegetation. Values less than 0.1 indicate no vegetation but barren area, rock, sand or snow (Tucker, 1979).

1.2. Monitoring vegetative drought

Monitoring vegetative drought usually requires a large amount of temporal data, and Remote Sensing (RS) technologies provide necessary means to collect these at regular intervals. NDVI is

* Corresponding author. Tel.: +31 53 4874559; fax: +31 53 4874400.
E-mail address: rulinda14348@itc.nl (C.M. Rulinda).

1569-8432/$ – see front matter © 2009 Elsevier B.V. All rights reserved.
doi:10.1016/j.jag.2009.10.008

commonly calculated using image data from polar orbiting satellites which carry sensors detecting radiation in red and infrared wavelengths. Despite their daily image data acquisitions, it may not be possible to obtain frequent cloud-free image data. In order to minimize the effects of clouds and atmospheric influence from aerosols and water vapor, temporal composites of 10 or 16 days are often used (Holben, 1986). The high temporal frequency of SEVIRI data increases the chance to obtain cloud-free images during a day and daily NDVI data is now more often available (Fensholt et al., 2006).

Vegetation conditions can be characterized by the deviation of the current NDVI values from their corresponding temporal mean NDVI values, usually calculated over a long period such as one or more decades. At each pixel site, this deviation, referred to in this paper as DV(t,s), is calculated as the difference between the current NDVI value and its corresponding time series mean, see Eq. (2) (Anyamba and Tucker, 2003).

$$\mathrm{DV}(t,s) = \mathrm{NDVI}(t,s) - \overline{\mathrm{NDVI}}(s) \tag{2}$$

where NDVI(t,s) is the current NDVI at site s and time t and $\overline{\mathrm{NDVI}}$ (s) is the mean NDVI value for different times, calculated for the time frame of the data series. When DV(t,s) is negative, it indicates below normal vegetation conditions and therefore suggests prevailing drought conditions; a large negative, persistent in time, corresponds with a severe drought. This indicator has been used and discussed in various studies (Anyamba and Tucker, 2003; Bajgiran et al., 2008).

1.3. Vegetative drought monitoring and uncertainties

Vegetation condition values, characterized by DV(t,s), are an interpretation of quantitative measurements of vegetation conditions. Drought classes are traditionally defined based on these quantitative measurements and modeled in geographic information systems (GIS) using traditional crisp classification techniques. This approach does not reflect the transition between the "drought" and "non-drought" classes. For drought, a gradual transition reflecting its severity is more appropriate. Moreover, at a location, the severity of drought depends not only on the intensity of vegetation stress but also on its duration (IWMI, 2008). Since vegetation stress caused by drought increases gradually over time, a hard spatial classification cannot discriminate potential information that can lead to a better understanding of drought onset and development. The coarse spatial resolution of SEVIRI data, equal to 3 km at the sub-satellite point, introduces further spatial uncertainties due to the mixture of land cover elements.

1.4. Image mining to monitor drought

Monitoring drought using remote sensing commonly requires a large time series of multi-spectral data. Image mining techniques (Stein, 2008) allow handling those and have been used in studies such as modeling of forest fires from Meteosat images (Umamaheshwaran et al., 2007) and using multi-sensor, multi-resolution data and multi-scale data (Tadesse et al., 2005). We propose an image mining approach to handle the large amount of data used in the processing of hourly NDVI images to obtain drought indicator metrics.

The aim of this study is to improve the early detection of drought using Meteosat SEVIRI data in eastern Africa. In doing so, combine image mining with the use of a membership function to process the large amount of image data and to account for uncertainties in the definition of vegetative drought. The drought spell in eastern Africa at the end of the year 2005 illustrates our approach.

2. Study area and study period

The eastern African region consists of nine countries usually divided geographically into sub-regions based on different types of vegetation, availability of water and topography. The continental sub-regions of eastern Africa include the Great Lakes Region and the Horn of Africa. Lakes and rivers are the main water sources in eastern Africa and where these are absent, sub-regions depend on rainfall. The first, more abundant rainy season is from around April to May and the second, more variable rainy season from around October to November (Hastenrath, 2001).

For this study, we selected a subset of images of eastern Africa, acquired for the months of September to December, between 2005 and 2007. The method was applied to the whole subset image data of eastern Africa, whereas eight crop field locations in drought prone areas of eastern Africa (see Fig. 1) are analyzed in more detail. The characteristics of these selected sites are presented in Table 1. Moreover, Fig. 1 shows three other locations ($L_{1,3}$) which are selected for the observation of NDVI diurnal variation. More details are given in Section 3.3.

Rainfall in Kenya is closely linked to the livelihoods of its citizens and the health of the nation's economy. For example, the La Niñ a drought of 1998–2000 caused damages such as the loss of hydropower and industrial production, the loss of crop and livestock, and with severe economic impacts, estimated at 16% of GDP in each of the 2 years. Since 98% of Kenya's cropping is rainfed, most farmers are exposed to the high variability of rainfall within and between years (WRI, 2007; Slegers, 2008). Rwanda's crop seasons are directly related to the two rainy seasons, with the first season running from September to December, followed by the second season from February to July. There is also a third marshland season that runs from June to September and October (MINAGRI, 2009). Rwanda is frequently confronted with incidences of drought, as a result of erratic and below average rainfall in the rainy seasons. Since agriculture is mostly dependent on rainfall, a reduction in the levels of precipitation has a direct

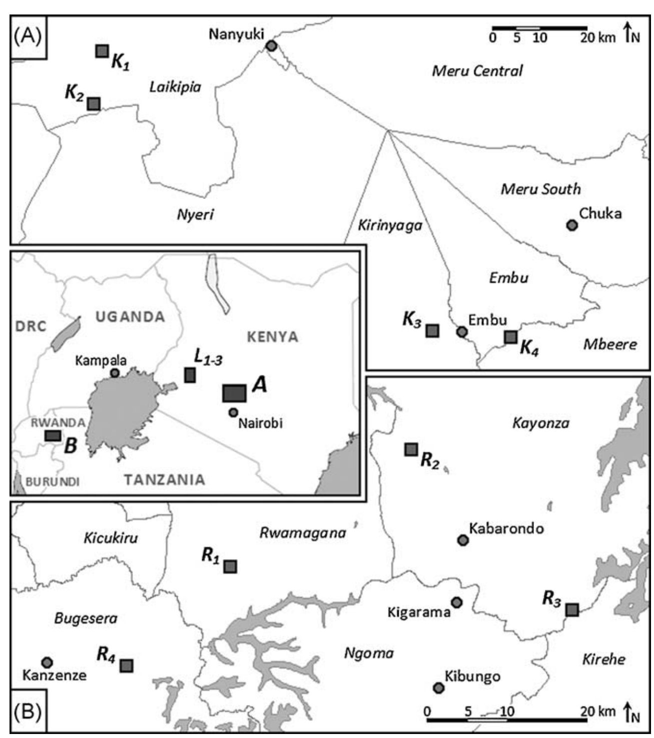

Fig. 1. Subset of eastern Africa with approximate locations of selected sites labeled as K_1 to K_4 in Kenya (A) and R_1 to R_4 in Rwanda (B) and L_1 to L_3.

Table 1
Land cover characteristics at the sites presented in Section 4 (WRI, 2007; Africover).

ID	Latitude	Longitude	Land cover type
k_1	0°0′0.00″N	36°46′0.00″E	Open shrub land (40–45% crown cover)
k_2	0°6′0.00″S	36°45′0.00″E	Rainfed herbaceous crop (clustered small fields with 35% crop intensity) with very sparse shrubs and trees
k_3	0°32′0.51″S	37°23′43.40″E	Scattered (in natural vegetation or other) rainfed herbaceous crop (field density 20–40%)
k_4	0°32′48.06″S	37°32′44.00″E	Scattered (in natural vegetation or other) rainfed herbaceous crop (field density 20–40%)
R_1	2°2′3.53″S	30°18′15.18″E	Combination of rainfed herbaceous crop, (40–60%) shrub plantation (20–40%) and natural vegetation
R_2	1°54′27.278″S	30°30′23.23″E	Combination of rainfed herbaceous crop, (20–40%) shrub plantation (40–60%) and natural vegetation
R_3	2°5′24.06″S	30°41′12.46″E	Combination of rainfed herbaceous crop, (20–40%) shrub plantation (40–60%) and natural vegetation
R_4	2°9′11.518″S	30°11′11.77″E	Combination of rainfed herbaceous crop, (20–40%) shrub plantation (40–60%) and natural vegetation
L_a	0°31′00.00″N	35°10′60.00″E	Rain fed herbaceous crop
L_b	0°21′00.00″N	35°24′60.00″E	Rain fed herbaceous crop
L_c	0°07′00.00″N	35°20′00.00″E	Forest plantation

impact on agricultural production. In general, the areas in Rwanda that are most prone to drought are the Central, Eastern and Southern regions of the country. From the end of 2005 to the beginning of 2006, parts of eastern Africa, such as in Rwanda FEWSN (2005a) and Kenya FEWSN (2005b) experienced droughts (FEWSN, 2006a).

3. Data acquisition and processing

3.1. The SEVIRI sensor and data

The first MSG satellite, Meteosat-8, was launched on August 29, 2002 at 3.3 ° West longitude at an altitude of 36,000 km. It became operational on January 29, 2004, and has since then recorded images of Europe, the North Atlantic and Africa with a temporal sampling of 15 min. The SEVIRI sensor is its main payload, equipped with 12 spectral channels, ranging from visible to far infrared wavelengths.

SEVIRI provides data to the European Organisation for the Exploitation of Meteorological Satellites (EUMETSAT) in Darmstadt, Germany. These data are processed and then uplinked to the HOTBIRD-6 communication satellite in wavelet compressed format. The International Institute for Geo-information Science and Earth Observation (ITC), in the Netherlands, receives and archives these data in compressed form on drivers accessible through personal computers on the network. Level 1.5 data were imported and converted into Ilwis raster data format using the MSG Data Retriever (Maathuis et al., 2005) tool available at ITC, with the aid of a Geospatial Data Abstraction Library (GDAL)-driver that reads raw compressed MSG data and facilitates easy geometric and radiometric calibrated data retrieval into formats commonly used by remote sensing packages.

In this study, bands one (*VIS 0.6*) (red, 0.56–0.71 μ m) and two (*VIS 0.8*) (near infrared, 0.74–0.88μ m), converted to reflectance have been used to calculate the NDVI. We used images covering the region during the crop season of September to December, for the years 2005, 2006 and 2007, recorded between 06:00 UTC and 11:00 UTC, corresponding approximately to 08:00–09:00 to 13:00–14:00 local time, respectively.

The cloud mask product (CLM) distributed by EUMETSAT is applied on each image. The NDVI values are calculated as in Eq. (1). No atmospheric correction was carried out.

3.2. Precipitation data

In this study we use precipitation data from August to November, 2005 to 2007, aggregated to 10-day period, to compare our with results. These data were taken from stations closest to the points selected for the drought analysis, i.e. respectively in Embu, Kenya and in Kigali, Rwanda. From Embu meteo station, k_1 is located at approximately 93 km, k_2 at 89 km, k_3 at 7.5 km and k_4 at 12 km. From Kigali meteo station, R_1 is located approximately at 21 km, R_2 at 42 km, R_3 at 63 km and R_4 at 23 km. Data for Embu were retrieved from the National Climatic Data Centre (NCDC, 2009) and data for Kigali from the Rwandan Meteorological Service. Precipitation data for Embu are incomplete in 2005 for the 1st, 2nd and 3rd dekad of August, and the 2nd dekad of November; in 2006 for the 3rd dekad of August, the 2nd dekad of September, the 2nd dekad of October and the 3rd dekad of November; and in 2007 for the 3rd dekad of October, and the 1st and 2nd dekad of November; as data for one or more days within these 10-day periods is missing. The data for the 2nd dekad of November have not been included in the chart of Fig. 3.

3.3. Generation of the DV(t,s) time series

We first conducted an observation of diurnal variation of NDVI on the 01st of July 2008 at three locations (L_1, L_2 and L_3) (see Table 1) in Kenya during a non-drought season. This particular day and these particular locations were selected based on the fact that most cloud-free scenes could be obtained. The NDVI was calculated at a 15-min interval. We assumed the observations as shown in Fig. 3 are valid for the eight study sites and as such considered a time window between 06:00 and 11:00 UTC (09:00 and 14:00 local time) to avoid including systematic low NDVI values. We then calculated the daily maximum NDVI composite for each of the selected sites. These daily NDVI composites were further used to generate the 4-day maximum NDVI composites. We first generated a daily NDVI time series by determining the maximum NDVI value from the available 15 min images during a 5 h observation window between 06:00 and 11:00 UTC, from September to December. This provided one daily value for these 4 months over a period of 3 years. To reduce the number of missing values in this series, we determined 4-day maximum NDVI composites, consisting in total of 90 values. Such a period of 4 days was selected as it was the minimum set with the least missing NDVI values. From the 4-day maximum values, we calculated the mean over 2005–2007 for each period of 4 days (30 values from September to December). To generate the DV(t,s) time series, we subtracted these means from the 4-day composite time series. Finally, we limited the series to the months of October and November in 2005, 2006 and 2007 ($n = 48$, DV(t,s)).

3.4. Spatial modeling of vegetative drought

To model drought from vegetation condition, we use fuzzy sets theory, thus accounting for the gradual transition between drought and non-drought classes modeling. *Fuzzy sets theory*, introduced by Zadeh (1984), provides a conceptual framework for solving knowledge representation and classification in an ambiguous environment. Elements of a fuzzy set can take values ranging from 0 to 1, unlike the traditionally used (Boolean) set whose elements take either 0 or 1. This function allows us to quantify the gradual

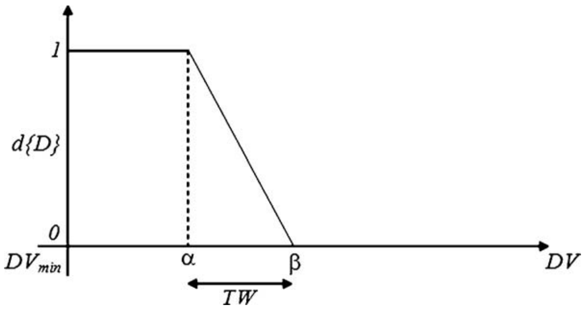

Fig. 2. Drought membership function $d\{D\}$ applied to DV.

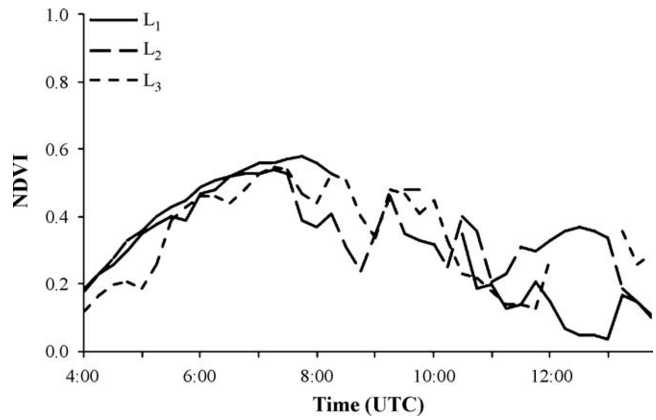

Fig. 3. Within-day variation of NDVI on July 1, 2008 at three selected sites s_a, s_b and s_c.

evolution of vegetative drought at a location. *Fuzzy sets theory* has been used and discussed in remote sensing studies of change detection analysis (Metternicht, 1999, 2001) and to model vague geographic entities (Fisher, 2000; Woodcock and Gopal, 2000; Cheng et al., 2009).

The parameters of the transition width (TW), which should be defined based on expert knowledge, were estimated arbitrarily in this study to illustrate the function. The shape of the function was selected on the basis of the following assumptions:

- Vegetation stress observed on DV(t,s) images is caused by drought condition.
- Variation of intensity of vegetation stress reflects linearly the variation of drought severity.
- Under natural conditions, the severity of vegetative drought evolves gradually in time.

Fig. 2 shows the shape of the membership function applied to DV(t,s) values. Where TW is the transition width limited by its lower limit α, and its upper limit β. DV_{min} is the overall minimum DV calculated during the study period.

$$d(D)\begin{cases} 1 & \forall x : x \le \alpha \\ \dfrac{\beta - x}{\beta - \alpha} & \forall x : \alpha < x < \beta \\ 0 & \text{otherwise} \end{cases} \tag{3}$$

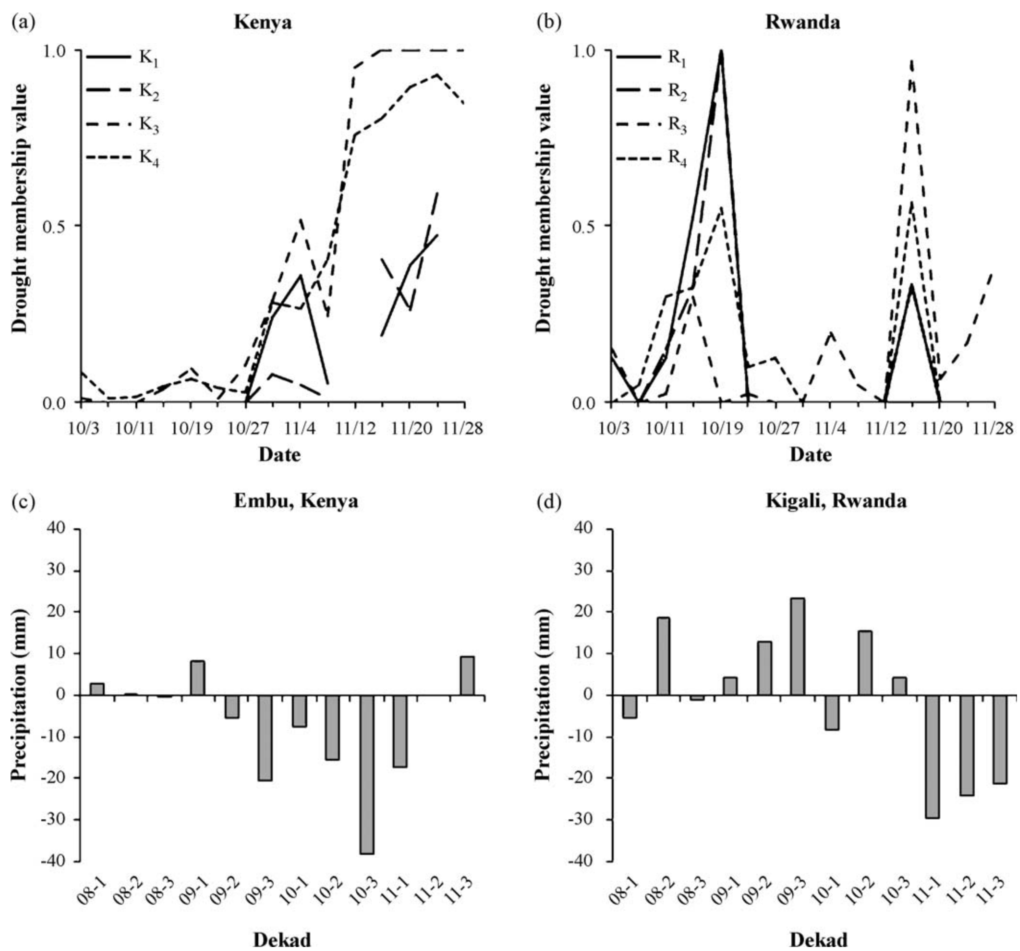

Fig. 4. (a) Drought membership variation at sites k_1, k_2, k_3 and k_4 (Embu region) from October to November 2005. (b) Drought membership variation at sites R_1, R_2, R_3 and R_4 (Kigali region) from October to November 2005. (c) Difference of precipitation in Embu (Kenya) from August to November 2005 with the mean precipitation calculated over the years 2005–2007. (d) Difference of precipitation in Kigali (Rwanda) from August to November 2005, with the mean precipitation calculated over the years 2005–2007.

The one-sided trapezoidal drought membership function, $d\{D\}$ as we defined in (3), takes the value 1 (or certain drought) for vegetation condition values below α and the value 0 (or certain non-drought) for vegetation condition values above β, with a gradual linear transition of drought membership values between 0 and 1, for vegetation condition values between α and β. The function was applied to the time series of DV(t,s). A few pixel locations in field crop areas of Kenya and Rwanda were extracted and tracked over time. Results are presented and discussed respectively in Sections 4 and 6.

4. Results

Fig. 3 shows the 15-min interval diurnal variation of NDVI at L_1, L_2 and L_3 on the 01st of July 2008. From the graph we observe an increase of NDVI values in the morning between approximately 04:00 and 07:00 UTC (07:00 and 10:00 local time), followed by a slow and gradual decline towards the evening.

Fig. 4(a) shows $d\{D\}$ values calculated at sites k_1 to k_4 in Kenya, for the period from October to November 2005, in a 4-day time scale, and Fig. 4(b) shows $d\{D\}$ values calculated at sites R_1 to R_4 in Rwanda, for the same period. The parameters $\alpha = -0.20$ and $\beta = 0$ were set for all sites. Fig. 4(c) and (d) are the precipitation difference values for August to November 2005, from the mean 2005–2007. We see that for Embu the increase in drought membership value coincides with less-than-average rainfall conditions, while this is not the case for Rwanda. In Fig. 4(a), we see for all sites a gradual increase of drought membership values from the end of October 2005 and in Fig. 4(d) a less-than-average amount of rainfall starting in the second dekad of September. In Fig. 4(b) we see for all sites a sharp increase of drought membership values from the beginning of October 2005, and a sharp decrease from the end of October. Drought membership values stay low to increase again sharply in mid-November. Fig. 4(d) shows an more-than-average amount of rainfall starting from the first dekad of September and a less-than-average amount of rainfall starting at the first dekad of November.

5. Sensitivity analysis

An S-shaped analytical function model (4) is proposed to fit the variation of drought membership values on time. This model contains two parameters a and b, reflecting the halfway point and the steepness of the function at that point, respectively. This function was fitted to both the membership functions with TW = 0.10 ($\alpha = -0.1$ and $\beta = 0$) and for those with TW = 0.20 ($\alpha = -0.1$ and $\beta = 0$) at the sites k_1 to k_4. Such a sensitivity analysis illustrates how the variation (uncertainty) in the output of the model can be apportioned quantitatively to the variation of input and parameters.

$$\frac{1}{\pi} \times \arctan\left(\frac{\text{date}}{b} - a\right) + 0.5 \tag{4}$$

Results of the fitting are shown in Table 2. From this table we consider a drought membership value of 0.1 as an early indicator for drought. Table 2 shows that for this membership value at sites k_1 to k_4, we observe a lag time on drought detection of approximately 13, 9, 8 and 4 days respectively, when increasing the TW from 0.10 to 0.20. A similar trend is observed for all other values of k_1 to k_4. The difference is largest for site k_1 where the detection of drought by a membership function is late (13.173 days after October 27th) and a change in one of the parameters of the membership function has the largest effect. This is consistent the slower and more gradual effect of drought in shrubland as compared with cropland. While annual crops and grasses are the first to be affected by drought, deeper rooting shrub and trees are more resilient and remain green throughout considerable periods of drought.

Table 2
Fitted coefficients a and b for Eq. (4) at the different sites, for $TW = 0.1$ and $TW = 0.20$. Included is the shift of the time where the fitted function takes the value 0.1.

Site	$\alpha = 0.10$			$\alpha = 0.20$			Shift (days)
		a	b	10%	a	b	10%
k_1	13.173	1.177	19.8	11.095	2.647	33.0	13.2
k_2	3.144	5.681	18.9	5.376	4.963	28.4	9.5
k_3	2.813	1.17	4.2	4.175	2.722	12.7	8.5
k_4	3.714	1.402	6.4	4.771	2.631	14.1	7.7

6. Discussion and conclusion

The study shows how to model drought indicators taking into account uncertainties related to the class definition of a drought. The shape of the drought membership distribution we obtained therefore depends entirely on vegetation condition, as measured from NDVI values. Further studies on combination of other external factors such as rainfall occurrence, irrigation or soil moisture conditions impacting vegetation condition will improve the accuracy of the proposed drought model.

The major strengths and weaknesses of the proposed approach pertain to both the generation of $d\{D\}(t, s)$ time series reflecting vegetation condition and the selection of the membership function. Due to the short lifetime of operation of SEVIRI, the time series mean values are computed for a limited period of 3 years, introducing errors in $d\{D\}(t, s)$ values. The strength of the use of a membership function compared to the traditional Boolean function to model drought, is that the gradual evolution of drought severity is taken into consideration. When vegetation stress is caused by another phenomenon than drought, such as human or animal induced stress, the changes of observed NDVI vegetation values, hence drought values, are not gradual but sharp. By using a membership function we might know when a change is more likely caused by natural drought conditions or by human activities. The approach that we used in this study to quantify drought can be used to optimize drought detection and remove false alarm. To do so we need to select the shape of the function as well as parameters α and β, which require an *a priori* knowledge of characteristics of vegetative drought at study sites. In this study, the shape of the function of the drought membership function and the parameters α and β have been chosen somewhat arbitrarily to illustrate our approach. Further research is needed to optimize the model.

A comparison with rainfall data was performed to assess the validity of the drought signal obtained, as NDVI is a response variable to rainfall. For Embu, increase in drought membership value coincided with less-than-average rainfall conditions, as expected, especially for the two locations (k_3 and k_4) closest to the Embu meteo station. However, for sites in eastern Rwanda, this was not the case. We suppose this could be caused by the large distance between Kigali meteo station and the four observation sites, or by the relied difference between Kigali, which is hilly and near the central Plateau, and the south-eastern part of Rwanda, which is flatter. As no rainfall data were available of areas closer to the observation sites, this assumption could not be validated.

The high temporal resolution data from instruments such as SEVIRI offers opportunities to address processes occurring in plants such as duration and intensity of photosynthetic activity and understanding of plant phenology which previously could not be measured. The exploitation of these parameters can provide additional information which can be beneficial in the context of drought monitoring; this is a potential area of investigation for future studies. Fensholt et al. (2006) suggested that the NDVI bowl-shaped curve observed from the variation of Meteosat-derived NDVI in Senegal during the morning can infer canopy structure. Bijker (2007) found similar results while observing diurnal NDVI variation in the Netherlands, however suggesting this pattern to be related to photosynthetic activity. From our observations during a day with predominant clear sky (results not included in the paper) we found similar bowl-shaped NDVI curves on selected sites in Kenya. Future research may reveal whether taking such effects into account leads to substantial improvement in drought modeling. Fensholt et al. (2006) observed peak values occurring around 10.45 local time and our test sites in Kenya showed peak values of NDVI at around 11 am local time (see Fig. 3). Future research in that area may also reveal whether taking such effects into account leads to substantial improvement in drought modeling.

A next step in drought modeling could also be an approach focusing on spatial objects. To do so, objects have to be built from collected images. Drought objects will be necessarily vague and uncertain, likely showing large spatial within-object variation as well. The method that we propose in this study may serve as a first step into this direction. In fact, what we have done here for individual pixels can also be done for a group of pixels. In principle, these pixels could be combined by considering a series of images into a 3-dimensional space-time drought object. Using an α-cut equal to 0.1 or 0.5 may then delineate the final objects. We see this as subsequent steps in this analysis.

Acknowledgements

The authors thank the Rwandan Meteorological Service for the provision of meteorological data. Useful suggestions from the anonymous reviewers are also gratefully acknowledged.

References

Anyamba, A., Tucker, C., 2003. Analysis of sahelian vegetation dynamics using NOAA-AVHRR NDVI data from 1981–2003. Journal of Arid Environment 63, 569–614.
Bajgiran, P., Darvishsefat, A., Khalili, A., Makhdoum, M., 2008. Using AVHRR-based vegetation indices for drought monitoring in the northwest of Iran. Journal of Arid Environments 72 (6), 1086–1096.
Barron, J., Rockstöm, J., Gichuki, F., Hatibu, N., 2003. Dry spell analysis and maize yields for two semi-arid locations in east Africa. Agriculture and Forest Meteorology 17, 23–37.
Bijker, W., July 2007. Diurnal variation in NDVI: implications for seasonal land long-term changes. In: 4th International workshop on the analysis of multi-temporal remote sensing images, Leuven, Belgium.
Cheng, T., Molenaar, M., Stein, A., 2009. Fuzzy approach for integrated costal zone management. Remote Sensing and Geospatial Technologies for Coastal Ecosystem Assessment and Management, Lecture Notes in Geoinformation and Cartography.
Cooper, P., Dimes, J., Rao, K., Shapiro, B., Twomlow, S., 2008. Coping better with current climatic variability in the rain-fed farming systems of sub-Saharan Africa: an essential first step in adapting to future climate change? Agriculture, Ecosystems & Environment 126 (1–2), 24–35.
Fensholt, R., Sandholt, I., Stisen, S., Tucker, C., 2006. Vegetation monitoring with the geostationary meteosat second generation seviri sensor. Remote Sensing of Environment 101, 212–229.
FEWSNET, 2005a. Rwanda food security update. Technical report. Famine Early Warning System Network (FEWSNET)
FEWSNET, 2005b. Kenya food security update. Technical report. Famine Early Warning System Network (FEWSNET).
FEWSNET, December 2005c. Africa: weather hazards assessment. Technical report. Famine early Warning System Network (FEWSNET).
FEWSNET, 2006a. Rwanda food security update. Technical report. Famine Early Warning System Network (FEWSNET).
FEWSNET, February 2006b. Africa: weather hazards assessment. Technical report. Famine early Warning System Network (FEWSNET).
Fisher, P., 2000. Sorites paradox and vague geographies. Fuzzy Sets and Systems 12, 47–62.
Hastenrath, S., 2001. Variations of east African climate during the past two centuries. Climate Change 50 (1–2), 209–217.
Herman, S., Anyamba, S., Tucker, C., 2005. Recent trends in vegetation dynamics in the African sahel and their relationship to climate. Global Environment Changes 15, 394–404.
Holben, B., 1986. Characteristics of maximum-value composite images for temporal AVHRR data. International Journal of Remote Sensing 7, 1435–1445.
IWMI, 2008. IWMI drought information center: understanding drought. Last accessed in February 2008.
Maathuis, B.H.P., Gieske, A.S.M., Restios, B., Hendrikse, J.H.M., Leeuwen, B., 2005. MSG data retriever: tool for converting raw MSG SEVIRI L 1.5 files into Raster-GIS or Raster image file format.
Metternicht, G., 1999. Change detection assessment using fuzzy sets and remotely sensed data: an application of topographic map revision. ISPRS Journal of Photogrammetry and Remote Sensing 54 (4), 221–223.
Metternicht, G., 2001. Assessing temporal and spatial changes of salinity using fuzzy logic, remote sensing and GIS. Foundations of an expert system. Ecological Modelling 144 (2–3), 163–179.
MINAGRI, 2009. Farming. Technical report. Ministry of Agriculture and Animal Resources, Rwanda.
Myneni, R., Asrar, G., 1994. Atmospheric effects and spectral vegetation indices. Remote Sensing of Environment 47 (3), 390–402.
NCDC, 2009. National climatic data centre. Last accessed in July 2009 (http://gis.ncdc.noaa.gov/website/ims-cdo/gsod/viewer.htm).
Nicholson, S., 1994. Recent rainfall fluctuations in Africa and their relationship to past conditions over the continent. The Holocene 4 (2), 121–134.
Nicholson, S., 2000. The nature of rainfall variability over Africa on time scales of decades to millenia. Global and Planetary Change 26, 137–158.
Olsson, L., Eklundh, L., Ardö, J., 2005. A recent greening of the sahel—trends, patterns and potential causes. Journal of Arid Environment 63, 556–566.
Slegers, M., 2008. "If only it would rain": farmers perceptions of rainfall and drought in semi-arid central Tanzania. Journal of Arid Environment 72, 2106–2123.
Stein, A., 2008. Modern developments in image mining. Science in China. Series E Technological Sciences 51 (Suppl. (1)), 13–25.
Swenson, S., Wahr, J., 2009. Monitoring the water balance of lake Victoria, east Africa, from space. Journal of Hydrology 370, 123–176.
Tadesse, T., Brown, J.F., Hayes, M.J.H., 2005. A new approach for predicting drought-related vegetation stress: integrating satellite, climate, and biophysical data over the U.S. central plains. ISPRS Journal of Photogrammetry and Remote Sensing 59 (4), 244–253.
Thorton, P., Jones, P., Alagarswamy, G., Andresen, J., 2009. Spatial variation of crop yield response to climate change in East Africa. Global Environmental Change 19, 54–65.
Tucker, C., 1979. Red and photographic infrared linear combinations for monitoring vegetations. Remote Sensing of Environment 8, 127–150.
Tucker, C., Stenseth, N.C., 2005. Using the satellite-derived NDVI to assess ecological responses to environmental change. Trends in Ecology & Evolution 20 (9), 503–510.
Umamaheshwaran, R., Bijker, W., Stein, A., 2007. Image mining for modeling of forest fires from meteosat images. IEEE Transactions on Geoscience and Remote Sensing 45 (1), 246–253.
Wilhite, D., 2005. Drought and water crisis: science, technology and management issues. Taylor & Francis Group.
Woodcock, E., Gopal, S., 2000. Fuzzy set theory and thematic maps: accuracy assessment and area estimation. International Journal of Geographical Information Science 14 (2), 153–172.
WRI, 2007. Nature's Benefits in Kenya. An Atlas of Ecosystems and Human Well-Being. World Resources Institute (WRI), Washington DC and Nairobi.
Zadeh, L., 1984. Fuzzy sets as a basis for a theory of possibility. Fuzzy Sets and Systems 1 (1), 3–28.